Magazine of Civil Engineering. 2019. 89(5). Pp. 61–78
Инженерно-строительный журнал. 2019. № 5(89). С. 61–78

Magazine of Civil Engineering

ISSN 2071-0305

journal homepage: http://engstroy.spbstu.ru/

DOI: 10.18720/MCE.89.6

# Finite element model of Reisner’s plates in stresses

***Yu.Ya. Tyukalov***
*Vyatka State University, Kirov, Russia*

**Keywords:** Reisner's plates, possible displacements, finite elements, bending plate

**Abstract.** A method for calculating bending plates by the finite element method based on Reisner's theory is proposed. The method is based on the fundamental principles of minimum of additional energy and possible displacements. For discretization of the subject area, arbitrary quadrangular finite elements are used. Over the area of the finite element, the moment fields and shear forces are approximated by constant functions that satisfy the differential equilibrium equations in the area of the finite element in the absence of a distributed load. Using the principle of possible displacements, algebraic equilibrium equations of the nodes of the finite element grid are compiled. In accordance with Reisner's theory, vertical displacements and angles of rotation of the middle surface of the plate are taken as nodal possible displacements as independent. The proposed method of calculation allows you to calculate both thick and thin plates. There is no effect of «locking» of the solution for thin plates, which is confirmed by calculations of rectangular plates with different support conditions of side and different ratios of thickness to plate sizes. The solutions obtained by the proposed method for plates of various shapes are compared with analytical solutions. Sufficiently fast convergence and accuracy of the proposed calculation method for both thick and thin plates is shown.

## *1. Introduction*

Bending plates are one of the main elements of the supporting structures for various construction objects. Often in construction, for example as a foundation, thick reinforced concrete slabs are used. When calculating thick plates, it is necessary to consider, in addition to bending deformations, transverse shear deformations of sections, which can significantly affect the stress-strain state of the plate. The theory of bending plates, based on the hypothesis of direct normals, does not allow to consider shear deformations. Finite elements, developed based on the Kirchhoff theory, can be used only for the calculation of thin plates [1–2].

The Reisner's bending plate theory is widely used for calculating thick plates [3–4]. In contrast to the classical Kirchhoff theory, in Reisner’s theory, the angles of rotation of the middle surface and vertical displacements are considered as independent variables. Such way makes it possible to lower the maximum order of derivatives in the strain energy functional and makes it possible to use first-order functions for approximating the displacement functions. As known, the direct use of Reisner’s theory for constructing finite elements in displacements leads to the «locking» effect which consists in the impossibility of using these finite elements for calculating thin plates, which limits their applicability only to the area of thick plates. In order to overcome the “blocking” effect, various additional coordination of the finite element’s unknowns is often used. For example, the hypothesis of direct normals is enforced gone at discrete points or high order shift theory is used [5–6]. The finite elements based on satisfying the hypothesis of direct normals in the middle of the sides of finite elements are widely used in software and demonstrate good accuracy.

Various variational principles are successfully used to solve the stability and dynamics problems of various structures, including plates of variable stiffness [7–8]. A detailed analysis of the applicability of variational principles to the solution of a wide range of problems of the theory of elasticity by the finite element method is performed in [9–10]. In these works, the formulations of the variational principles of Lagrange,

Tyukalov, Yu.Ya. Finite element model of Reisner’s plates in stresses. Magazine of Civil Engineering. 2019. 89(5). Pp. 61–78. DOI: 10.18720/MCE.89.6

Тюкалов Ю.Я. Конечно-элементная модель в напряжениях для пластин Рейснера // Инженерно-строительный журнал. 2019. № 5(89). С. 61–78. DOI: 10.18720/MCE.89.6

Castilian, Reisner are considered in detail and the relevance of obtaining a two-sided estimate of the obtained approximate solutions is noted.

When constructing analytical solutions of the problems of bending rectangular plates, high-order shear theories are applied. In this case, along the cross section the deformations change according to law different from linear principle [11–12]. To construct finite elements that consider shear deformations, the third-order shear theory is applied successfully [13–14]. In [14], quadrangular finite element is presented that has seven degrees of freedom at each node: three displacements of the middle surface along the axes of coordinates, two shear angles and two angles of rotation of the normals. Such an approach allows one to more accurately consider shear deformations, when the properties of the material are changing in different directions. In [15], an additional procedure is used to account for shear deformations in the finite elements already construct, which are used to calculate thin plates. Transverse shear deformations are calculated of based on the direct application of the equations of the three-dimensional theory of elasticity. To construct quadrangular finite element the Galerkin's method is used in a weak form [16]. Also, the Galerkin's method is used to construct triangular and quadrangular finite elements according to Reisner-Mindlin theory in [17]. In [18, 19], analytical solutions for rectangular plates, obtained based on Reisner's theory, are proposed.

Mixed and hybrid variational formulations are also used to construct finite elements of plates with allowance for shear deformations [20–23]. On the one hand, such formulations simplify the inclusion of shear deformations by using both displacements and shear forces and moments as unknowns, but, on the other hand, matching of displacements and forces is required to ensure convergence.

Thus, most of the developed methods for calculating plates with considering shearing deformations, in one form or another, are based either on approximations of displacement functions or on solving differential equations expressed in terms of displacement functions. In this case, stresses are determined as derivatives of displacements expressed by approximate functions, which leads to an inevitable loss of accuracy in their determination, although stresses are more important for assessing the strength of a structure. In addition, the accuracy of the solution depends on the selected finite element mesh and we cannot, in the general case for an arbitrary construction, determine the accuracy of the solution obtained. Therefore, it remains actual to build alternative models, to the finite element method in displacements, for considering shear deformations when calculating flexible plates based on Reisner's theory. If we have solutions obtained on an alternative basis, then by comparing two (or more) solutions we will be able to obtain a more reliable estimate of the accuracy of the solutions obtained.

The purpose of this work is to develop a method for calculating plates with considering to the shear deformations of Reisner's plates, which based on the functional of additional energy and the principle of possible displacements, as well as comparing the solutions obtained for plates of various shapes and with different supporting conditions with solutions obtained by other methods. Such an approach for solving the plane problem of the theory of elasticity is used in [24], for rod systems in [25–26] and for bendable plates in [27–28]. In [28], a method for calculating thick bent plates with allowance for shear deformations based on the extended Castiliano functional is proposed. As additional terms, using the Lagrange multipliers method, algebraic equilibrium equations of nodes, obtained using the principle of possible displacements, are added to the functional. Possible vertical displacements of nodes causing bending and possible vertical displacements of nodes causing shear are used separately. As a result of the calculation, the rotation angles for the nodes are not directly determined. In this work, as possible displacements, both possible displacements in the form of vertical displacements and rotation angles will be used. In this case, as a result of the calculation, we can obtain both the magnitudes of the vertical displacements and the magnitudes of the rotation angles, which is more convenient.

## 2. Methods

Solving the problems of plate bending we obtain based on the functional of additional energy for an isotropic plate (for simplicity, we assume that there are no specified displacements) considering the shear deformations:

$$\Pi^{c} = \frac{1}{2}\left(\frac{12}{E \cdot t^{3}}\right)\int\left(M_x^2 + M_y^2 - 2\nu M_x M_y + 2\left(1+\nu\right)M_{xy}^2\right)\mathrm{d}\Omega + \frac{1}{2}\left(\frac{2k\left(1+\nu\right)}{E \cdot t}\right)\int\left(Q_x^2 + Q_y^2\right)\mathrm{d}\Omega \rightarrow \min. \quad (1)$$

$E$ is the modulus of material elasticity;

$t$ is the plate thickness;

$\nu$ is Poisson's ratio;

$k$ = 6/5 is coefficient considering the parabolic law of change of tangential stress across the plate thickness. The functional (1) is can written in matrix form that is more convenience for solving by the finite element method:

$$\Pi^c = \frac{1}{2}\int \{M\}^T [E]^{-1} \{M\} \mathrm{d}\Omega + \frac{1}{2}\int \{Q\}^T [E_{sh}]^{-1} \{Q\} \mathrm{d}\Omega \to \min. \tag{2}$$

In expression (2) the following notation is entered:

$$\{M\} = \begin{Bmatrix} M_x \\ M_y \\ M_{xy} \end{Bmatrix}, \quad \{Q\} = \begin{Bmatrix} Q_x \\ Q_y \end{Bmatrix}, \quad [E]^{-1} = \frac{12}{E \cdot t^3} \begin{bmatrix} 1 & -\nu & 0 \\ -\nu & 1 & 0 \\ 0 & 0 & 2(1+\nu) \end{bmatrix}, \quad [E_{sh}]^{-1} = \frac{12(1+\nu)}{5E \cdot t} \begin{bmatrix} 1 & 0 \\ 0 & 1 \end{bmatrix}. \tag{3}$$

In functional (2), the first addend is associated with the bending deformations of the plate, the second is due to shear deformations by transverse forces.

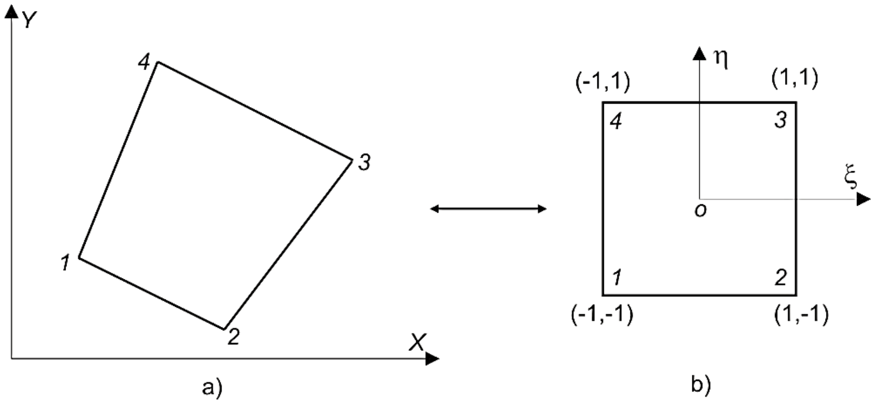


**Figure 1. An arbitrary quadrangular finite element.**

For discretization of the subject area, we use arbitrary quadrangular finite elements (Figure 1). Over the area of the finite element the moments and shear forces will be approximated by the constant functions. It is obvious that such functions satisfy differential equilibrium equations in the area of a finite element in the absence of distributed loads.

For the finite element $k$ in the global coordinate system, we combine the unknown internal forces into the vector $\{F_k\}$, and shall denote the flexible matrix as $[D_k]$.

$$\{F_k\} = \begin{Bmatrix} M_{x,k} \\ M_{y,k} \\ M_{xy,k} \\ Q_{x,k} \\ Q_{y.k} \end{Bmatrix}, \quad [D_k] = A_k \begin{bmatrix} \frac{12}{E \cdot t^3} & \frac{-12 \cdot \nu}{E \cdot t^3} & 0 & 0 & 0 \\ \frac{-12 \cdot \nu}{E \cdot t^3} & \frac{12}{E \cdot t^3} & 0 & 0 & 0 \\ 0 & 0 & \frac{24(1+\nu)}{E \cdot t^3} & 0 & 0 \\ 0 & 0 & 0 & \frac{12(1+\nu)}{5 \cdot E \cdot t} & 0 \\ 0 & 0 & 0 & 0 & \frac{12(1+\nu)}{5 \cdot E \cdot t} \end{bmatrix}. \tag{4}$$

$A_k$ is the area of the finite element;

$n$ is number of finite elements. Then the expression of the functional (1) can be written in the following matrix form:

$$\Pi^c = \frac{1}{2}\sum_{k=1}^{n} \{F_k\}^T [D_k] \{F_k\} = \frac{1}{2}\{F\}^T [D] \{F\} \to \min; \tag{5}$$

$$[D] = \begin{bmatrix} [D_1] & & \\ & \ddots & \\ & & [D_n] \end{bmatrix}, \quad \{F\} = \begin{Bmatrix} \{F_1\} \\ \vdots \\ \{F_n\} \end{Bmatrix}. \tag{6}$$

In accordance with the principle of minimum of the additional energy, the functions for moments $M_x$, $M_y$, $M_{xy}$ and shear forces $Q_x$, $Q_y$ must satisfy the corresponding differential equilibrium equations (7) and static boundary conditions.

$$\frac{\partial M_x}{\partial x}+\frac{\partial M_{xy}}{\partial y}-Q_x=0,\quad \frac{\partial M_y}{\partial y}+\frac{\partial M_{xy}}{\partial x}-Q_y=0,\quad \frac{\partial Q_x}{\partial x}+\frac{Q_y}{\partial y}+q=0. \tag{7}$$

Dividing the region of problem into finite elements and using approximations for internal efforts, then we shall obtain a finite-dimensional analog of the differential equations (7). For this we use the method of weighted residuals. Then for the first differential equation, we can write the following equations for the method of weighted residuals:

$$\int_{A_i}\left(\frac{\partial M_x}{\partial x}+\frac{\partial M_{xy}}{\partial y}-Q_x\right)\delta\theta_{x,i}\mathrm{d}A=0,\quad i=1,2,\ldots N. \tag{8}$$

$N$ is the number of nodes of the finite element grid;

$\delta\theta_{x,i}$ is weight functions;

$A_i$ is area of the region where the weight function is nonzero. We assume that the weight functions $\delta\theta_{x,i}$ are nonzero only in the region of finite elements adjacent to the node $i$ under consideration. Such weight functions can be called "local" or "finite". Using for (8) the integration procedure in parts, we obtain the following expression:

$$-\int_{A_i}\left(M_x\frac{\partial\left(\delta\theta_{x,i}\right)}{\partial x}+M_{xy}\frac{\partial\left(\delta\theta_{x,i}\right)}{\partial y}-Q_x\delta\theta_{x,i}\right)dA+\int_{A_i}\left(\frac{\partial\left(M_x\delta\theta_{x,i}\right)}{\partial x}+\frac{\partial\left(M_{xy}\delta\theta_{x,i}\right)}{\partial y}\right)dA=0,\ i=1,2,\ldots,N. \tag{9}$$

The second integral in expression (9) can be transformed using the Gauss theorem [1] (integration by parts in the plane case) into the integral over the boundary of the region, then we get:

$$\int_{A_i}\left(M_x\frac{\partial\left(\delta\theta_{x,i}\right)}{\partial x}+M_{xy}\frac{\partial\left(\delta\theta_{x,i}\right)}{\partial y}-Q_x\delta\theta_{x,i}\right)dA-\int_{\Gamma_i}\left(M_xl_x+M_{xy}l_y\right)\delta\theta_{x,i}\mathrm{d}\Gamma=0,\ i=1,2,\ldots,N. \tag{10}$$

$\Gamma_i$ is the boundary of the area in which the weight function $\delta\theta_{x,i}$ is nonzero;

$l_x, l_y$ are direction cosines of normal to the boundary of the region $\Gamma_i$. If we shall give the weight functions $\delta\theta_{x,i}$ a physical meaning and take them in the form of possible angles of rotation along the $X$ axis, then expression (10) coincides with the expression of the principle of possible displacements. The first integral in (10) is the work of internal forces on possible displacements, the second integral is the potential of external, given moments on the boundary. Bending and torsional moments perform work on the corresponding curvatures, and shear forces perform work on shear angles.

Performing similar transformations to the second and third equations (7), we obtain two more equilibrium equations:

$$\int_{A_i}\left(M_y\frac{\partial\left(\delta\theta_{y,i}\right)}{\partial y}+M_{xy}\frac{\partial\left(\delta\theta_{y,i}\right)}{\partial x}-Q_y\delta\theta_{y,i}\right)dA-\int_{\Gamma_i}\left(M_yl_y+M_{xy}l_x\right)\delta\theta_{y,i}d\Gamma=0,\ i=1,2,\ldots,N. \tag{11}$$

$$\int_{A_i}\left(Q_x\frac{\partial\left(\delta w_i^{sh}\right)}{\partial x}+Q_y\frac{\partial\left(\delta w_i^{sh}\right)}{\partial y}\right)dA-\int_{\Gamma_i}\left(Q_xl_x+Q_yl_y\right)\delta w_i^{sh}d\Gamma-\int_{A_i}q\delta w_i^{sh}\mathrm{d}A=0,\ i=1,2,\ldots,N. \tag{12}$$

$\delta\theta_{y,i}$ is possible displacement (weight function) in the form of a rotation angle along the $Y$ axis;

$\delta w_i^{sh}$ is possible displacement (weight function) in the form of a vertical displacement associated with a shear.

Thus, from differential equilibrium equations (7), for the Reisner plate, we obtained algebraic equilibrium equations (10)–(12) for nodes of the finite elements grid, which, when crushing the grid, will tend to differential equations. Note that expressions for derivatives of internal forces are not included in expressions (2), (10)–(12), so they can be accepted to be constant over the finite element region, and possible displacements can be taken as linear functions.

To build a solution, instead of the three differential equilibrium equations (7), having completed the transformations, we can get only two:

$$\frac{\partial^2 M_x}{\partial x^2}+2\frac{\partial^2 M_{xy}}{\partial x \partial y}+\frac{\partial^2 M_y}{\partial y^2}+q=0,\ \frac{\partial Q_x}{\partial x}+\frac{Q_y}{\partial y}+q=0. \tag{13}$$

Obviously, the first equation is associated with bending deformations, and the second with shear deformations. For the second differential equation, algebraic equilibrium equations (12) are obtained above. For the first equation, we shall take the function $\delta w_i^b$ as a weight function. Then we get

$$\int_{A_i}\left(\frac{\partial^2 M_x}{\partial x^2}+2\frac{\partial^2 M_{xy}}{\partial x \partial y}+\frac{\partial^2 M_y}{\partial y^2}+q\right)\delta w_i^b dA=0,\ i=1,2,\dots,N. \tag{14}$$

For the convenience of recording transformations, we introduce intermediate notation:

$$\delta\varphi_{x,i}=\frac{\partial w_i^b}{\partial x},\ \delta\varphi_{y,i}=\frac{\partial w_i^b}{\partial y},\ V_x=\frac{\partial M_x}{\partial x},\ V_y=\frac{\partial M_y}{\partial y},\ U_x=\frac{\partial M_{xy}}{\partial x},\ U_y=\frac{\partial M_{xy}}{\partial y}. \tag{15}$$

Using (15) we get

$$\int_{A_i}\left(\frac{\partial V_x}{\partial x}+\frac{\partial U_x}{\partial y}+\frac{\partial U_y}{\partial x}+\frac{\partial V_y}{\partial y}+q\right)\delta w_i^b dA=0,\ i=1,2,\dots,N. \tag{16}$$

Let us demonstrate the further transformations scheme by the example of the transformation of the first addend in (16). Using procedure of integration in parts we get:

$$I_1=\int_{A_i}\frac{\partial V_x}{\partial x}\delta w_i^b dA=-\int_{A_i}V_x\frac{\partial\left(\delta w_i^b\right)}{\partial x}dA+\int_{A_i}\frac{\partial\left(V_x\delta w_i^b\right)}{\partial x}dA. \tag{17}$$

Next, using the Gauss theorem, we replace the second integral over the area by the integral along the boundary contour:

$$I_1=-\int_{A_i}V_x\frac{\partial\left(\delta w_i^b\right)}{\partial x}dA+\int_{\Gamma_i}V_x l_x\delta w_i^b d\Gamma. \tag{18}$$

Using (15), we replace the variables again:

$$I_1=-\int_{A_i}\frac{\partial M_x}{\partial x}\delta\varphi_{x,i}dA+\int_{\Gamma_i}\frac{\partial M_x}{\partial x}l_x\delta w_i^b d\Gamma. \tag{19}$$

To the first integral from (19), we also use integration by parts:

$$I_1=\int_{A_i}M_x\frac{\partial\left(\delta\varphi_{x,i}\right)}{\partial x}dA-\int_{A_i}\frac{\partial\left(M_x\delta\varphi_{x,i}\right)}{\partial x}dA+\int_{\Gamma_i}\frac{\partial M_x}{\partial x}l_x\delta w_i^b d\Gamma. \tag{20}$$

Applying the Gauss theorem to the second integral, we finally get

$$I_1=\int_{A_i}M_x\frac{\partial^2\left(\delta w_i^b\right)}{\partial x^2}dA-\int_{\Gamma_i}M_x l_x\frac{\partial\left(\delta w_i^b\right)}{\partial x}d\Gamma+\int_{\Gamma_i}\frac{\partial M_x}{\partial x}l_x\delta w_i^b d\Gamma. \tag{21}$$

Using similar transformations for all terms and using the expression for the transverse forces from (7), we obtain the following expression for (16):

$$\int\limits_{A_i}\left(M_x\frac{\partial^2\left(\delta w_i^b\right)}{\partial x^2}+2M_{xy}\frac{\partial^2\left(\delta w_i^b\right)}{\partial x\partial y}+M_y\frac{\partial^2\left(\delta w_i^b\right)}{\partial y^2}\right)dA-\int\limits_{\Gamma_i}\left(M_x l_x+M_{xy}l_y\right)\frac{\partial\left(\delta w_i^b\right)}{\partial x}d\Gamma$$
$$-\int\limits_{\Gamma_i}\left(M_y l_y+M_{xy}l_x\right)\frac{\partial\left(\delta w_i^b\right)}{\partial y}d\Gamma+\int\limits_{\Gamma_i}\left(Q_x l_x+Q_y l_y\right)\delta w_i^b d\Gamma+\int\limits_{A_i}q.\delta w_i^b dA=0,\ \ i=1,2,\ldots,N. \quad (22)$$

Equations (22) are equilibrium equations for nodes on possible vertical displacements, causing flexural deformations. In [27, 28], equilibrium equations like (22) were used in constructing a solution for Kirchhoff plates, which based on the functional of additional energy. Linear functions were taken as possible displacements in the finite element region. Therefore, in the triangular finite elements, the first integral was zero. For the rectangular finite elements in the first integral, only the term associated with the torsional curvature was nonzero. The fourth integral is zero, both at the boundaries between the finite elements and at the outer boundaries. The fourth integral is the work of transverse forces normal to the boundary. Therefore, if the external boundary is free, then the transverse forces are zero. If there are no displacements at the border, then there is also zero the possible displacement. The second and third integrals in (22) are the work of moments at the angles of rotation along the normal to the sides of the finite elements. With linear possible displacements, these angles get fractures (breaks) and therefore the third and fourth integrals will not be equal to zero. In papers [27, 28] for triangular finite elements, these integrals were calculated using geometric constructions. Note that when using this approach to the solution, it is impossible to use the approximations of forces constant over the finite element region, since in this case the second and third integrals will be equal to zero.

Comparing the two options have considered above, we note that in the second version, the states of bending and shear are completely separated, and in the first version they are connected. But at the same time, it should be noted that the original differential equations equilibrium of are the same.

In this paper, we will use the first version of the equilibrium equations construction, based on three independent possible displacements. In accordance with the minimum of additional energy principle the functions of moments and shear forces must satisfy the corresponding differential equilibrium equations and static boundary conditions. Since, in the general case, it is almost impossible to select such functions, we shall act as follows. Using the possible displacements principle, we shall compose algebraic equilibrium equations for the nodes of the finite element grid. In this case, in accordance with Reisner's theory we shall take, as the nodal possible displacements, the vertical displacements and rotation angles of middle surface independently. Further, the resulting algebraic equilibrium equations will be added to the functional (5) using the Lagrange multipliers method. This ensures the equilibrium of the selected stress fields in a discrete sense (in nodes) and the solution can be obtained by minimizing the resulting extended functional. It should be noted that the number of equilibrium equations must be less than the total number of unknown nodal forces. Since the forces in the domain of finite elements are approximated by constant functions, then small grids are necessary for obtaining sufficiently accurate solutions, therefore the above requirement will be fulfilled. For example, in a 4×4 square grid, the number of unknown nodal forces will already be greater than the number of equilibrium equations, even if the superposed supports are not taken into account.

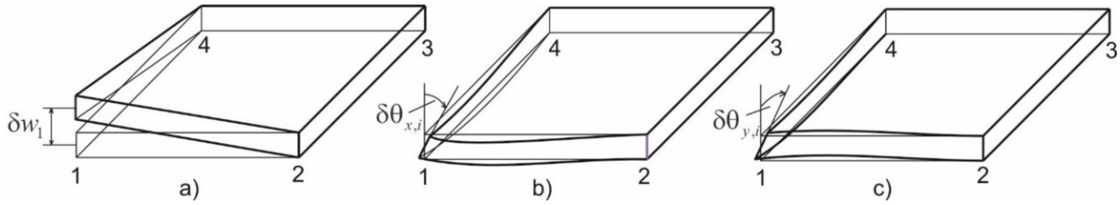


**Figure 2. Possible displacements of the node 1 of finite element.**

To get the solution, we use the well-known transformation of an arbitrary quadrilateral (Figure 1a) into the square element (Figure 1b). Such transformation can be written in the following form:

$$x=\sum\nolimits_{i=1}^{4}N_i(\xi,\eta)\cdot x_{i,k},\quad y=\sum\nolimits_{i=1}^{4}N_i(\xi,\eta)\cdot y_{i,k},\quad N_i(\xi,\eta)=\frac{1}{4}(1+\xi_i\xi)(1+\eta_i\eta). \quad (23)$$

$x_{i,k}$, $y_{i,k}$ are coordinates nodes of finite element $k$ in the global coordinate system.

Displacements in the finite element area, caused by possible displacements of the node $i$, we shall express using the linear basis functions introduced above – $N_i(\xi,\eta)$:

$$\delta w = N_i(\xi,\eta)\delta w_i, \quad \delta\theta_x = N_i(\xi,\eta)\delta\theta_{x,i}, \quad \delta\theta_y = N_i(\xi,\eta)\delta\theta_{y,i}. \tag{24}$$

With the possible displacement $\delta w_i = 1$ only shear deformations occur in the plate:

$$\delta\gamma_{xz} = \frac{\partial(\delta w)}{\partial x} = \frac{\partial N_i(\xi,\eta)}{\partial x}, \quad \delta\gamma_{yz} = \frac{\partial(\delta w)}{\partial y} = \frac{\partial N_i(\xi,\eta)}{\partial y}. \tag{25}$$

Then, the work of the internal forces of finite element $k$ by possible displacement is expressed in the following form:

$$\delta U_{w_i,k} = Q_{x,k}\iint_{A_k}\delta\gamma_{xz}dA + Q_{y,k}\iint_{A_k}\delta\gamma_{yz}dA. \tag{26}$$

The work of external forces

$$\delta V_{w_i,k} = P_{z,i} + \iint_{A_r} N_i(\xi,\eta)\cdot q_{z,k}dA. \tag{27}$$

$P_{z,i}$ is force which concentrated in a node;

$q_{z,k}$ is load which is distributed over area of the finite element;

$A_k$ is area of the finite element. In accordance with the principle of possible displacements, we shall obtain the equilibrium equation for the node $i$

$$\sum_{k\in\Xi_i}\delta U_{w_i,k} + \sum_{k\in\Xi_i}\delta V_{w_i,k} = 0. \tag{28}$$

$\Xi_i$ is the set of finite elements adjacent to the node $i$. Equations (28) for all nodes can be written in the following general matrix form:

$$\{C_{w,i}\}^T\{F_{w,i}\} + \overline{P}_i = 0, \quad i\in\Xi_w. \tag{29}$$

$\{C_{w,i}\}$ is vector containing the coefficients before unknown forces of finite elements in the equilibrium equation of the node $i$;

$\{F_{w,i}\}$ is vector of unknown forces of finite elements adjacent to node $i$.

$\overline{P}_i$ is generalized force equal to the work of external forces;

$\Xi_w$ is set of nodes that have degree of freedom along the $Z$ axis. The expressions for the elements of the vectors and the generalized forces will be given below.

With the possible displacement in the form of rotation angle along the $X$ axis $\delta\theta_{x,i} = 1$, both bending and torsional deformations and shear deformations take place:

$$\delta\chi_{xx} = \frac{\partial(\delta\theta_x)}{\partial x} = \frac{\partial N_i(\xi,\eta)}{\partial x}, \quad \delta\chi_{xy} = \frac{\partial(\delta\theta_x)}{\partial y} = \frac{\partial N_i(\xi,\eta)}{\partial y}, \quad \delta\gamma_{xz} = -\delta\theta_x = -N_i(\xi,\eta). \tag{30}$$

In this case, the work of the internal forces for the finite element has the following form:

$$\delta U_{\theta_{xi},k} = Q_{x,k}\iint_{A_k}\delta\gamma_{xz}dA + M_{x,k}\iint_{A_k}\delta\chi_{xx}dA + M_{xy,k}\iint_{A_k}\delta\chi_{xy}dA. \tag{31}$$

The work of external forces in the general case

$$\delta V_{\theta_{xi},k} = M_{\theta_x,i} + \iint_{A_r} N_i(\xi,\eta)\cdot m_{\theta_x,k}dA. \tag{32}$$

$M_{\theta_x,i}$ is the moment of external forces concentrated in the node, which acting along the $X$ axis; – acting along the $X$ axis moment of external forces, which distributed over the finite element area;

$A_k$ is the area of the finite element. Equilibrium equation, like equation (29), will have the following form:

$$\left\{C_{\theta_x,i}\right\}^T \left\{F_{\theta_x,i}\right\} + \bar{M}_{x,i} = 0, \quad i \in \varXi_{\theta_x}. \tag{33}$$

$\left\{C_{\theta_x,i}\right\}$ is vector containing coefficients before unknown forces of finite elements in the equilibrium equation of the node $i$;

$\left\{F_{\theta_x,i}\right\}$ is unknown forces vector for finite elements adjacent to node $i$.

$\bar{M}_{x,i}$ is generalized moment equal to the work of external forces;

$\Xi_{\theta_x}$ is nodes set, which have degrees of freedom in the form turn angles $\theta_x$.

For possible displacement, in the form a rotation angle along the $Y$ axis $\delta\theta_{y,i} = 1$, such expressions are written similarly:

$$\delta\chi_{yy} = \frac{\partial(\delta\theta_y)}{\partial y} = \frac{\partial N_i(\xi,\eta)}{\partial y}, \quad \delta\chi_{xy} = \frac{\partial(\delta\theta_y)}{\partial x} = \frac{\partial N_i(\xi,\eta)}{\partial x}, \quad \delta\gamma_{yz} = -\delta\theta_y = -N_i(\xi,\eta). \tag{34}$$

$$\delta U_{\theta_{yi},k} = Q_{y,k}\iint_{A_k}\delta\gamma_{yz}dA + M_{y,k}\iint_{A_k}\delta\chi_{yy}dA + M_{xy,k}\iint_{A_k}\delta\chi_{xy}dA. \tag{35}$$

$$\delta V_{\theta_{yi},k} = M_{\theta_y,i} + \iint_{A_r} N_i(\xi,\eta)\cdot m_{\theta_y,k}dA. \tag{36}$$

$$\left\{C_{\theta_y,i}\right\}^T \left\{F_{\theta_y,i}\right\} + \bar{M}_{y,i} = 0, \quad i \in \Xi_{\theta_y}. \tag{37}$$

Using the Lagrange multipliers, equations (29), (33) and (37) we shall add to the functional (5). Then we get

$$\varPi^c = \frac{1}{2}\{F\}^T[D]\{F\} + \sum_{i\in\varXi_w} w_i\left(\left\{C_{w,i}\right\}^T\left\{F_{w,i}\right\} + \bar{P}_i\right) +$$
$$\sum_{i\in\varXi_{\theta_x}} \theta_{x,i}\left(\left\{C_{\theta_x,i}\right\}^T\left\{F_{\theta_x,i}\right\} + \bar{M}_{x,i}\right) + \sum_{i\in\varXi_{\theta_x}} \theta_{y,i}\left(\left\{C_{\theta_y,i}\right\}^T\left\{F_{\theta_y,i}\right\} + \bar{M}_{y,i}\right) \to \min. \tag{38}$$

We introduce the notation for the nodal displacements global vector – $\{W\}$. The vector combines all unknown vertical displacement and rotation angles for the whole area:

$$\{W\} = \begin{pmatrix} w_1 & \theta_{x,2} & \theta_{y,3} & \cdots & w_{m-2} & \theta_{x,m-1} & \theta_{y,m}\end{pmatrix}^T.$$

Then, equating to zero the derivatives of the functional (38) with respect to the vectors $\{W\}$ and $\{F\}$, we shall obtain the following linear algebraic equations system:

$$\begin{bmatrix} [D] & [L]^T \\ [L] & [0] \end{bmatrix}\begin{Bmatrix} \{F\} \\ \{W\} \end{Bmatrix} = \begin{Bmatrix} \{P\} \\ 0 \end{Bmatrix}. \tag{39}$$

The matrix $[L]$ and vector $\{P\}$ is formed from the coefficients of the equilibrium equations (29), (33) and (37).

The matrix $[D]$ is block diagonal form and easily analytically invertible. Therefore, we can express the vector $\{F\}$ from first matrix equation:

$$\{F\} = [D]^{-1}\{P\} - [D]^{-1}[L]^T\{W\} \tag{40}$$

Then we express the vector $\{W\}$ from the second matrix equation

$$[K]\{W\} = [D]^{-1}\{P\}, \quad [K] = [L][D]^{-1}[L]^T. \tag{41}$$

Note that the matrix $[K]$ has tape structure of nonzero elements.

Consider the matrix $[L]$ formation algorithm for a plate represented by arbitrary quadrangular finite elements. For partial derivatives of the function $N_i(\xi,\eta)$ of the finite element with the number $k$, the following expressions can be written:

$$\frac{\partial N_i}{\partial \xi}=\frac{\partial N_i}{\partial x}\frac{\partial x}{\partial \xi}+\frac{\partial N_i}{\partial y}\frac{\partial y}{\partial \xi},\quad \frac{\partial N_i}{\partial \eta}=\frac{\partial N_i}{\partial x}\frac{\partial x}{\partial \eta}+\frac{\partial N_i}{\partial y}\frac{\partial y}{\partial \eta}. \tag{42}$$

Index $i$ denotes the local number of a finite element node (Figure 1a). Equations (42) are written in the matrix form:

$$\begin{Bmatrix}\dfrac{\partial N_i}{\partial \xi}\\ \dfrac{\partial N_i}{\partial \eta}\end{Bmatrix}=\begin{bmatrix}\dfrac{\partial x}{\partial \xi} & \dfrac{\partial y}{\partial \xi}\\ \dfrac{\partial x}{\partial \eta} & \dfrac{\partial y}{\partial \eta}\end{bmatrix}\begin{Bmatrix}\dfrac{\partial N_i}{\partial x}\\ \dfrac{\partial N_i}{\partial \eta}\end{Bmatrix},\quad [J]=\begin{bmatrix}\dfrac{\partial x}{\partial \xi} & \dfrac{\partial y}{\partial \xi}\\ \dfrac{\partial x}{\partial \eta} & \dfrac{\partial y}{\partial \eta}\end{bmatrix}. \tag{43}$$

Using relations (7), we obtain the expressions of the Jacobi $[J]$ matrix's elements:

$$\begin{aligned}
J_{11}&=\frac{\partial x}{\partial \xi}=\sum_{i=1}^{4}\frac{\xi_i\left(1+\eta\eta_i\right)}{4}x_{i,k}=\frac{1}{4}\left[\left(1-\eta\right)\left(x_{2,k}-x_{1,k}\right)+\left(1+\eta\right)\left(x_{3,k}-x_{4,k}\right)\right],\\
J_{12}&=\frac{\partial y}{\partial \xi}=\sum_{i=1}^{4}\frac{\xi_i\left(1+\eta\eta_i\right)}{4}y_{i,k}=\frac{1}{4}\left[\left(1-\eta\right)\left(y_{2,k}-y_{1,k}\right)+\left(1+\eta\right)\left(y_{3,k}-y_{4,k}\right)\right],\\
J_{21}&=\frac{\partial x}{\partial \eta}=\sum_{i=1}^{4}\frac{\eta_i\left(1+\xi\xi_i\right)}{4}x_{i,k}=\frac{1}{4}\left[\left(1-\xi\right)\left(x_{4,k}-x_{1,k}\right)+\left(1+\xi\right)\left(x_{3,k}-x_{2,k}\right)\right],\\
J_{22}&=\frac{\partial x}{\partial \eta}=\sum_{i=1}^{4}\frac{\eta_i\left(1+\xi\xi_i\right)}{4}y_{i,k}=\frac{1}{4}\left[\left(1-\xi\right)\left(y_{4,k}-y_{1,k}\right)+\left(1+\xi\right)\left(y_{3,k}-y_{2,k}\right)\right].
\end{aligned} \tag{44}$$

From relation (43), we can obtain the expressions for the necessary derivatives:

$$\begin{Bmatrix}\dfrac{\partial N_i}{\partial x}\\ \dfrac{\partial N_i}{\partial \eta}\end{Bmatrix}=[J]^{-1}\begin{Bmatrix}\dfrac{\partial N_i}{\partial \xi}\\ \dfrac{\partial N_i}{\partial \eta}\end{Bmatrix},\quad [J]^{-1}=\begin{bmatrix}b_{11} & b_{12}\\ b_{21} & b_{22}\end{bmatrix}. \tag{45}$$

The elements of matrix $[J]^{-1}$ have the following expressions:

$$\det J=J_{11}J_{22}-J_{12}J_{21},\quad b_{11}=\frac{J_{22}}{\det J},\quad b_{12}=\frac{-J_{12}}{\det J},\quad b_{21}=\frac{-J_{21}}{\det J},\quad b_{22}=\frac{J_{11}}{\det J}. \tag{46}$$

Using the expression (45) and (7), we shall get

$$\begin{aligned}
\frac{\partial N_i}{\partial x}&=b_{11}\frac{\xi_i\left(1+\eta\eta_i\right)}{4}+b_{12}\frac{\eta_i\left(1+\xi\xi_i\right)}{4},\\
\frac{\partial N_i}{\partial y}&=b_{21}\frac{\xi_i\left(1+\eta\eta_i\right)}{4}+b_{22}\frac{\eta_i\left(1+\xi\xi_i\right)}{4}.
\end{aligned} \tag{47}$$

We shall get integrals on the area of arbitrary quadrilateral finite element, for function $N_i(\xi,\ \eta)$ and it derivatives $\frac{\partial N_i}{\partial x}$, $\frac{\partial N_i}{\partial y}$, using the integrals on area of square element.

$$\begin{aligned}
c_{1i,k}&=\iint_{A_k}\frac{\partial N_i}{\partial x}dA=\frac{1}{4}\int_{-1}^{1}\int_{-1}^{1}\left(b_{11}\xi_i\left(1+\eta\eta_i\right)+b_{12}\eta_i\left(1+\xi\xi_i\right)\right)\det J\,d\xi d\eta,\\
c_{2i,k}&=\iint_{A_k}\frac{\partial N_i}{\partial y}dA=\frac{1}{4}\int_{-1}^{1}\int_{-1}^{1}\left(b_{21}\xi_i\left(1+\eta\eta_i\right)+b_{22}\eta_i\left(1+\xi\xi_i\right)\right)\det J\,d\xi d\eta,\\
c_{3i,k}&=\iint_{A_k}N_i dA=\frac{1}{4}\int_{-1}^{1}\int_{-1}^{1}\left(1+\xi\xi_i\right)\left(1+\eta\eta_i\right)\det J\,d\xi d\eta.
\end{aligned} \tag{48}$$

Integrals (48) are calculated numerically using the four-point Gauss formula.

Using (48), we write the expressions (26), (31) and (35) for the possible displacements of the node $i$ for the finite element with the number $k$ in the following form:

$$\begin{aligned} \delta U_{w_i,k} &= Q_{x,k}c_{1i,k} + Q_{y,k}c_{2i,k}, \\ \delta U_{\theta_{xi},k} &= M_{x,k}c_{1i,k} + M_{xy,k}c_{2i,k} - Q_{x,k}c_{3i,k}, \\ \delta U_{\theta_{yi},k} &= M_{xy,k}c_{1i,k} + M_{y,k}c_{2i,k} - Q_{y,k}c_{3i,k}. \end{aligned} \tag{49}$$

We can introduce the vector – $\{\delta U_{i,k}\} = \begin{Bmatrix} \delta U_{w_i,k} \\ \delta U_{\theta_{xi},k} \\ \delta U_{\theta_{yi},k} \end{Bmatrix}$. Then

$$\{\delta U_{i,k}\} = [L_{i,k}]\{F_k\}, \quad [L_{i,k}] = \begin{bmatrix} 0 & 0 & 0 & c_{1i,k} & c_{2i,k} \\ c_{1i,k} & 0 & c_{2i,k} & -c_{3i,k} & 0 \\ 0 & c_{2i,k} & c_{1i,k} & 0 & -c_{3i,k} \end{bmatrix}. \tag{50}$$

From the matrices $[L_{i,k}]$ formed for each finite elements nodes, in accordance with the numbering of the nodes and finite elements, the global matrix $[L]$ is formed for whole system. If the boundary of the area is not parallel to one of the global axes, but lies at an angle $\alpha$ to the $X$ axis, then the matrix should be multiplied by the matrix of direction cosines:

$$[L_{i,k}^s] = [S][L_{i,k}], \quad [S] = \begin{bmatrix} 1 & 0 & 0 \\ 0 & \cos\alpha & \sin\alpha \\ 0 & -\sin\alpha & \cos\alpha \end{bmatrix}. \tag{51}$$

For the case of a load uniformly distributed on the finite element, the work of external forces on possible displacement is calculated by the following formula:

$$\delta V_{w_i,k} = \iint_{A_r} N_i(\xi,\eta)\cdot q_{z,k}\mathrm{d}A = q_{z,k}c_{3i,k}. \tag{52}$$

## *3. Results and Discussion*

It is well known that when using the theory of bending of Reisner plates for building finite elements in the form of the displacement's method, the so-called problem of “locking” the solution arises. “Locking” is that such finite elements are unsuitable for the calculation of thin plates. Therefore, as first example, we shall obtain solutions for rectangular plates with different ratios of the plate thickness to its dimensions and for different variants of supporting the sides (Figure 3).

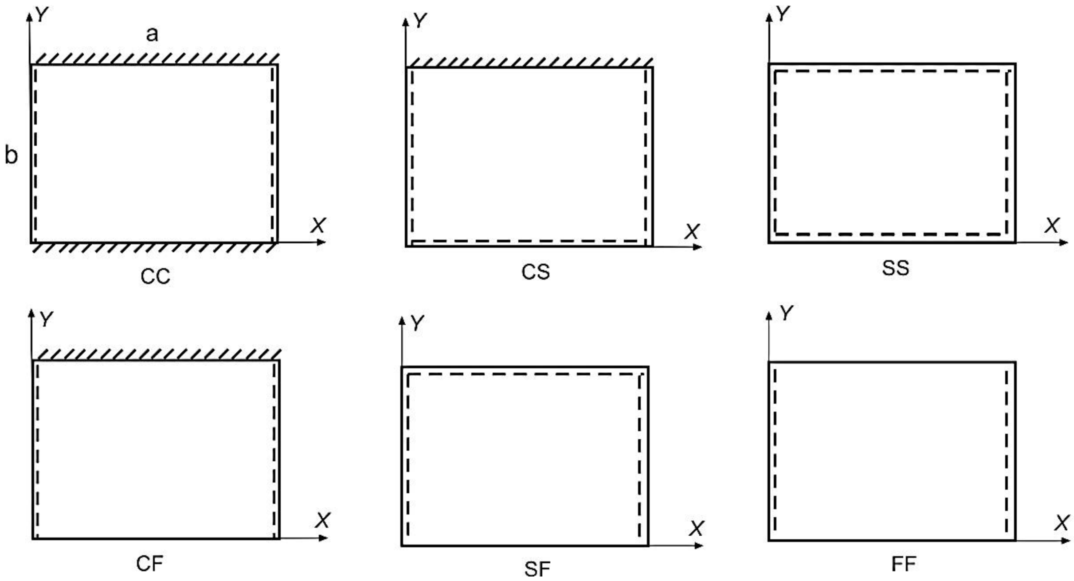


**Figure 3. Conditions of support and the sizes of the sides of bending Levi's plates.**

In Figure 3 dashed line and the letter S denotes a simply supported side, the oblique hatching and the letter C denotes a clamped side, and the letter F denotes the free side. Table 1 presents the results of calculations of the plate denoted SS, given in [11] for various theories, and the results obtained by the proposed method — SFEM. The lengths of the plate sides were taking equal to 3 m or 1.5 m. The side 3 m long was divided into 30 finite elements, and the side 1.5 m — into 16 elements. Poisson's ratio is $\nu = 0.3$. The load was taken evenly distributed over the plate area. The results of calculations in Table 1 are presented in dimensionless form:

$$\overline{w} = \frac{100D}{qa^4} w\left(\frac{a}{2}, \frac{b}{2}\right). \tag{53}$$

***Table 1. Displacement of the center of the plate under the action of a uniformly distributed load.***

| $a$ | $b$ | $t/a$ | Theory | Boundary conditions | | | | | |
|---|---|---|---|---|---|---|---|---|---|
| | | | | CC | CS | SS | CF | SF | FF |
| 3 | 1.5 | 0.001 | CRT | 0.0163 | 0.0305 | 0.0633 | 0.1450 | 0.3810 | 1.3714 |
| | | | S-FSDT | 0.0163 | 0.0305 | 0.0633 | 0.1450 | 0.3809 | 1.3713 |
| | | | [11] | 0.0163 | 0.0305 | 0.0633 | 0.1450 | 0.3810 | 1.3714 |
| | | | **SFEM** | **0.0161** | **0.0303** | **0.0632** | **0.1449** | **0.3808** | **1.3688** |
| | | 0.04 | CRT | 0.0178 | 0.0322 | 0.0647 | 0.1505 | 0.3880 | 1.3797 |
| | | | S-FSDT | 0.0175 | 0.0318 | 0.0646 | 0.1476 | 0.3835 | 1.3770 |
| | | | [11] | 0.0178 | 0.0322 | 0.0646 | 0.1504 | 0.3879 | 1.3795 |
| | | | **SFEM** | **0.0176** | **0.0320** | **0.0646** | **0.1503** | **0.3890** | **1.3769** |
| | | 0.1 | CRT | 0.0256 | 0.0421 | 0.0725 | 0.1746 | 0.4111 | 1.4168 |
| | | | S-FSDT | 0.0245 | 0.0386 | 0.0714 | 0.1614 | 0.3972 | 1.4070 |
| | | | [11] | 0.0256 | 0.0407 | 0.0714 | 0.1721 | 0.4084 | 1.4130 |
| | | | **SFEM** | **0.0254** | **0.0405** | **0.0715** | **0.1721** | **0.4100** | **1.4103** |
| | | 0.2 | CRT | 0.0524 | 0.0694 | 0.0958 | 0.2391 | 0.4688 | 1.5247 |
| | | | S-FSDT | 0.0489 | 0.0630 | 0.0958 | 0.2105 | 0.4464 | 1.5141 |
| | | | [11] | 0.0525 | 0.0695 | 0.0958 | 0.2395 | 0.4692 | 1.5248 |
| | | | **SFEM** | **0.0524** | **0.0695** | **0.0960** | **0.2396** | **0.4712** | **1.5220** |
| 3 | 3 | 0.001 | CRT | 0.1917 | 0.2785 | 0.4062 | 0.5667 | 0.7931 | 1.3094 |
| | | | S-FSDT | 0.1917 | 0.2786 | 0.4062 | 0.5667 | 0.7931 | 1.3094 |
| | | | [11] | 0.1917 | 0.2786 | 0.4062 | 0.5667 | 0.7931 | 1.3094 |
| | | | **SFEM** | **0.1916** | **0.2786** | **0.4063** | **0.5663** | **0.7924** | **1.3068** |
| | | 0.04 | CRT | 0.1965 | 0.2830 | 0.4096 | 0.5737 | 0.7981 | 1.3154 |
| | | | S-FSDT | 0.1955 | 0.2819 | 0.4096 | 0.5712 | 0.7975 | 1.3151 |
| | | | [11] | 0.1965 | 0.2830 | 0.4096 | 0.5737 | 0.7981 | 1.3154 |
| | | | **SFEM** | **0.1964** | **0.2834** | **0.4107** | **0.5732** | **0.7983** | **1.3128** |
| | | 0.1 | CRT | 0.2209 | 0.3059 | 0.4273 | 0.6065 | 0.8224 | 1.3459 |
| | | | S-FSDT | 0.2128 | 0.2996 | 0.4273 | 0.5945 | 0.8208 | 1.3451 |
| | | | [11] | 0.2209 | 0.3059 | 0.4273 | 0.6065 | 0.8224 | 1.3459 |
| | | | **SFEM** | **0.2209** | **0.3065** | **0.4289** | **0.6061** | **0.8230** | **1.3432** |
| | | 0.2 | CRT | 0.3021 | 0.3827 | 0.4904 | 0.7139 | 0.9072 | 1.4539 |
| | | | S-FSDT | 0.2759 | 0.3827 | 0.4904 | 0.6777 | 0.9041 | 1.4523 |
| | | | [11] | 0.3021 | 0.3827 | 0.4904 | 0.7139 | 0.9072 | 1.4539 |
| | | | **SFEM** | **0.3023** | **0.3837** | **0.4924** | **0.7135** | **0.9081** | **1.4512** |
| 1.5 | 3 | 0.001 | CRT | 0.8445 | 0.9270 | 1.0129 | 1.0605 | 1.1496 | 1.2887 |
| | | | S-FSDT | 0.8445 | 0.9270 | 1.0129 | 1.0605 | 1.1496 | 1.2887 |
| | | | [11] | 0.8445 | 0.9270 | 1.0129 | 1.0605 | 1.1496 | 1.2887 |
| | | | **SFEM** | **0.8440** | **0.9256** | **1.0106** | **1.0564** | **1.1444** | **1.2804** |
| | | 0.04 | CRT | 0.8511 | 0.9330 | 1.0181 | 1.0664 | 1.1547 | 1.2938 |
| | | | S-FSDT | 0.8497 | 0.9322 | 1.0181 | 1.0660 | 1.1551 | 1.2944 |
| | | | [11] | 0.8511 | 0.9330 | 1.0181 | 1.0664 | 1.1547 | 1.2938 |
| | | | **SFEM** | **0.8506** | **0.9323** | **1.0172** | **1.0623** | **1.1502** | **1.2855** |
| | | 0.1 | CRT | 0.8850 | 0.9637 | 1.0454 | 1.0981 | 1.1829 | 1.3228 |
| | | | S-FSDT | 0.8770 | 0.9596 | 1.0454 | 1.0946 | 1.1837 | 1.3244 |
| | | | [11] | 0.8850 | 0.9637 | 1.0454 | 1.0981 | 1.1829 | 1.3228 |
| | | | **SFEM** | **0.8845** | **0.9638** | **1.0420** | **1.0940** | **1.1791** | **1.3145** |
| | | 0.2 | CRT | 1.0000 | 1.0704 | 1.1430 | 1.2090 | 1.2844 | 1.4283 |
| | | | S-FSDT | 0.9746 | 1.0572 | 1.1430 | 1.1970 | 1.2861 | 1.4316 |
| | | | [11] | 1.0000 | 1.0704 | 1.1430 | 1.2090 | 1.2844 | 1.4283 |
| | | | **SFEM** | **0.9998** | **1.0712** | **1.1446** | **1.2050** | **1.2812** | **1.4199** |

The results presented in Table 1 demonstrate good accuracy of the solution according to the proposed method, both for thin and thick plates. Thus, the proposed solution method is free from the so-called “locking” effect and can be used to calculate plates of any thickness.

To assess the accuracy of determining the bending moments, we consider the results of calculations of the SS plate for different aspect ratios. It is known that when the sides of plate are simply supported, the values of the bending moments don't depend on the plate thickness. Table 2 provides comparison of the values of moments in the center of the plate, obtained by the proposed method, with the results of analytical calculations according to the Kirchhoff theory [29]. The finite element grid was taken 21×21.

***Table 2. Moments in the center of the SS plate which loaded with a uniformly distributed load.***

| $b/a$ | $100M_x/qa^2$ | | | $100M_y/qa^2$ | | |
|---|---|---|---|---|---|---|
| | $t/a$ = 0.001 | $t/a$ = 0.2 | Exact [29] | $t/a$ = 0.001 | $t/a$ = 0.2 | Exact [29] |
| 1.0 | 4.79 | 4.84 | 4.79 | 4.79 | 4.84 | 4.79 |
| 1.1 | 5.55 | 5.60 | 5.54 | 4.93 | 4.98 | 4.93 |
| 1.2 | 6.27 | 6.33 | 6.27 | 5.01 | 5.06 | 5.01 |
| 1.3 | 6.94 | 7.00 | 6.94 | 5.03 | 5.08 | 5.03 |
| 1.4 | 7.55 | 7.62 | 7.55 | 5.02 | 5.07 | 5.02 |
| 1.5 | 8.11 | 8.19 | 8.12 | 4.98 | 5.03 | 4.98 |
| 1.6 | 8.62 | 8.69 | 8.62 | 4.93 | 4.98 | 4.92 |
| 1.7 | 9.08 | 9.15 | 9.08 | 4.86 | 4.90 | 4.86 |
| 1.8 | 9.48 | 9.56 | 9.48 | 4.78 | 4.83 | 4.79 |
| 1.9 | 9.85 | 9.92 | 9.85 | 4.71 | 4.75 | 4.71 |
| 2.0 | 10.17 | 10.24 | 10.17 | 4.63 | 4.67 | 4.64 |

Note that for thin plates, the proposed solution practically coincides with the analytical one, and for thick plates one, the resulting moments are more than analytical ones by about 1 %.

Also, the rate of the solution convergence by the proposed method was tested when was crushing the finite element grid. The test showed fast convergence of displacements for all considered variants of plates. In Figure 4 shows graphs of solutions convergence for two variants of square plates, depending on the number side's divisions.

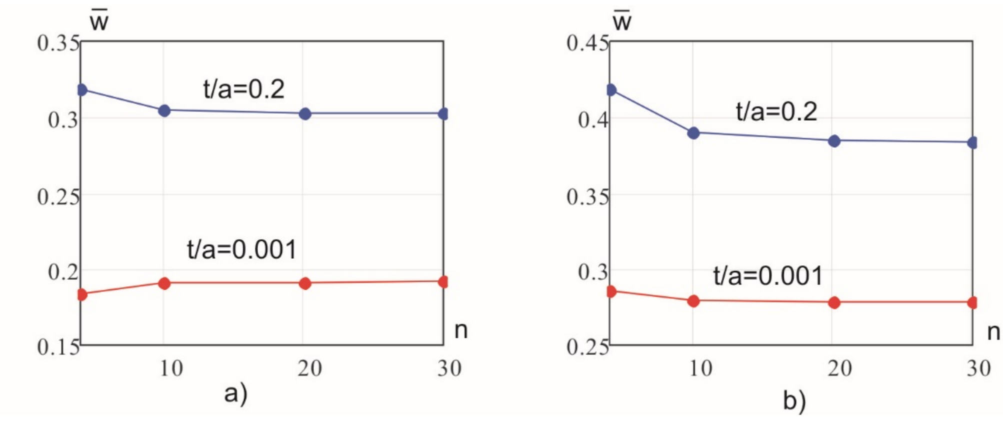


**Figure 4. Displacement the center of a square plate depending on the number of side divisions: a) SS plate; b) CS plate.**

In Figure 5 shows the graphs of the change in bending moments in the SS plate (Figure 3) for various sides ratios. The plate was crushed into 21 finite elements along each side. Therefore, the lengths of the finite element’s sides were in the same ratio as the lengths of the plate sides. Bending moments are constant values in the finite element region and so more accurately model the value in the finite element centers. Therefore, to more accurately determine the value of the moment in the clamped side middle $M_{y,2}$, linear extrapolation was used according to the moment values in the two finite elements nearest to the boundary. Obviously, with an increase in the ratio of the finite element sides, the error in determining the moment on the clamped side also increases.

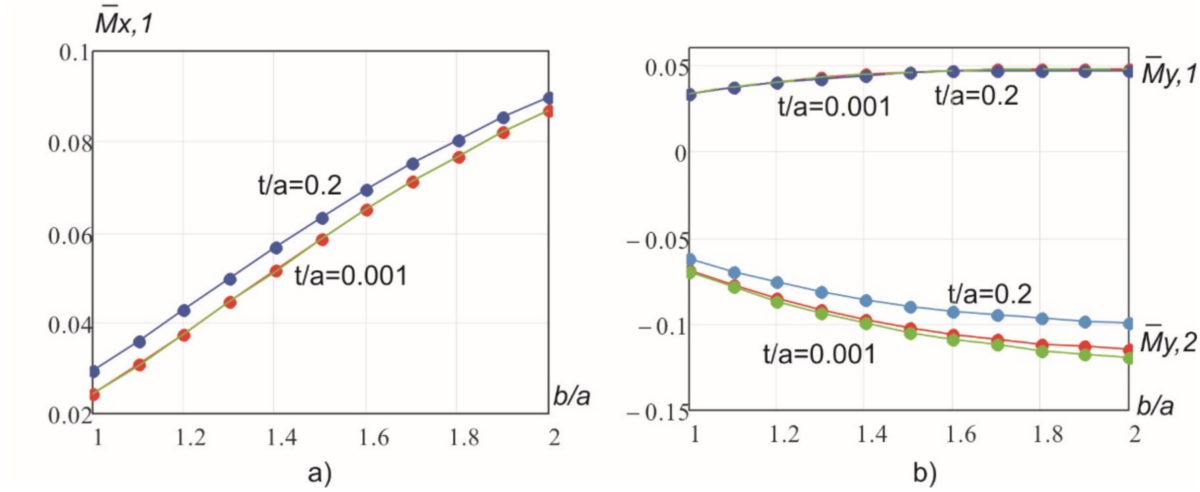


**Figure 5. Bending moments for a uniformly loaded square plate CC with different ratios of sides. $\bar{M}_{x,1} = M_{x,1}/qa^2$ and $\bar{M}_{y,1} = M_{y,1}/qa^2$ are bending moments in the center of the plate; $\bar{M}_{y,2} = M_{y,2}/qa^2$ is bending moment in the middle of the clamped side. Designations: Red line is $t/a$ = 0.001; Blue line is $t/a$ = 0.2; Green line is the solutions for the Kirchhoff plate [29].**

Graphs in Figure 5 shows the concurrence of the obtained moment values for thin plates with the analytical solution for Kirchhoff plates (the Green lines coincide with the Red lines). For thick plates (Blue line), only the moments $\bar{M}_{y,1}$ coincide with the solution for Kirchhoff's plates (Figure 5b). The values of the moments $\bar{M}_{x,1}$ and $\bar{M}_{y,2}$ for thick plates differ by 10–20 % from the corresponding moments obtained for thin plates. For an additional estimation of the results accuracy obtained, square SS plate was calculated on the LIRA-SAPR program using volume finite elements. A quarter of the plate was divided into 12 elements in height and into 20 elements along the X and Y axes. A plate with thickness $t$ = 0.6m was calculated. The dimensions of the plate quarter in plan are 1.5 m by 1.5 m. Poisson's ratio $\nu$ = 0.3. Load is $q$ = 10 kN/m². Modulus of elasticity is $E$ = 10000 kN/m².

***Table 3. Stresses in a square SS plate – (Figure 2).***

| Solution | Fiber of section | Center of the plate | | Middle of the clamped side |
|---|---|---|---|---|
| | | $\lvert\sigma_{x,1}\rvert, kN/m^2$ | $\lvert\sigma_{y,1}\rvert, kN/m^2$ | $\lvert\sigma_{y,2}\rvert, kN/m^2$ |
| LIRA-SAPR | top | 41.85 | 43.39 | 88.11 |
| | bottom | 47.50 | 46.29 | 89.13 |
| | mean value | 44.68 | 44.84 | 88.62 |
| SFEM | | 43.91 | 49.95 | 93.15 |
| Kirchhoff's plate [29] | | 36.54 | 49.86 | 103.46 |

Comparison of the results presented in Table 3 shows that the stress values obtained for thick plate based on Reisner's theory agree well with the stress values obtained by solving three-dimensional elasticity theory problem. Stresses in the clamped side $\sigma_{y,2}$ were determined using linear extrapolation from the values in the two finite elements nearest to the boundary. Also note that the displacements of the slab center, obtained by the LIRA-SAPR program, are 8.5 % more than the displacements obtained by the proposed method.

As next example the semiring was calculated on the acting of uniformly distributed load (Figure 6). The semiring has hinge supports along the lines DE and DB, and clamped support along the line EA. Line AB is the axis of symmetry, therefore, in the nodes lying on this line, the angles of rotation along the horizontal axis were excluded. In the calculations were taken the following data: $E$ = 10000 kN/m², $\mu$ = 0.3, $t$ = 0.1 m, $q$ = 10 kN/m², $R$ = 6 m, $r$ = 3 m. In Figure 7 shows graphs of changes along the line AB: bending radial moments – $\bar{M}_y$; moments directed perpendicular to the line AB – $\bar{M}_x$ and vertical displacements $\bar{w}$.

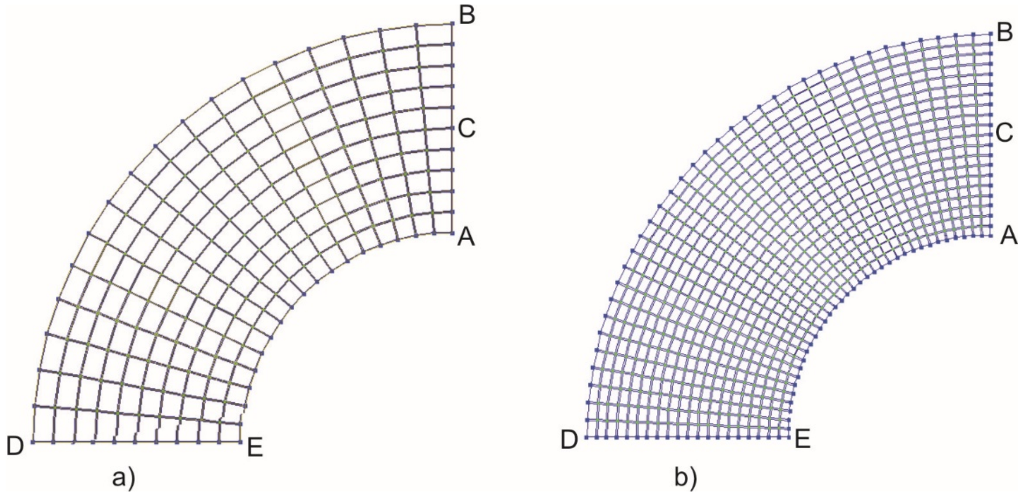


**Figure 6. Finite element grids of the ring quarter.**

$$\overline{w} = w\frac{1000D}{qR^4}, \overline{M}_x = \frac{M_x}{qR^2}, \overline{M}_y = \frac{M_y}{qR^2}. \tag{54}$$

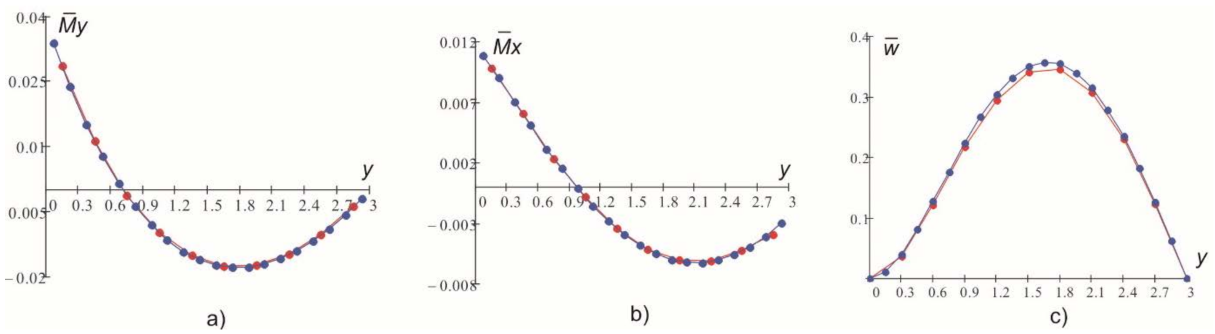


**Figure 7. Bending moments and deflections of the semiring along the AB line:**
**Red line is scheme in Figure 6a; Blue line is scheme in Figure 6b.**

***Table 4. Comparison of calculation results for the semiring with an analytical solution.***

| Solution | $\overline{w}_c$ | $\overline{M}_{x,C}$ | $\overline{M}_{y,C}$ | $\overline{M}_{x,A}$ | $\overline{M}_{y,A}$ |
|---|---|---|---|---|---|
| SFEM (Figure 6б) | 0.357 | 0.0118 | 0.0387 | –0.00436 | –0.0167 |
| Analytical [30] | 0.358 | 0.0118 | 0.0393 | –0.00439 | –0.0168 |

The values of the moments at point C were determined as the middle value of moments in two finite elements adjacent to the point on both sides. The values of the moments at point A were determined by linear extrapolation from the values of moments in the two nearest finite elements. Graphs in Figure 7 illustrate the linear variation of moments near clamped side ($y$ = 0). Thus, the graphs in Figure 7 and the data in Table 4 show good convergence and accuracy of the proposed method and for this example.

In the following example we use the finite element in the form of a parallelogram which have maximum inner angle of 120 degrees. A skewed plate was calculated (Figure 8). For such plate the finite difference solution is given in [29].

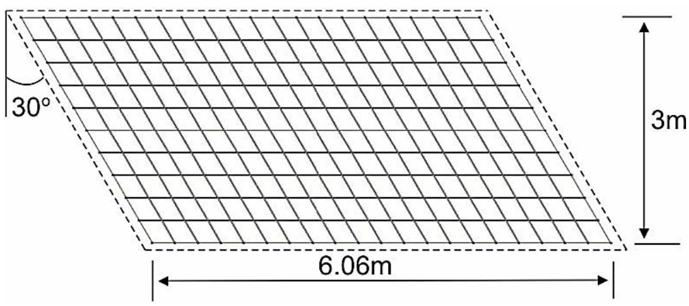


**Figure 8. Skewed plate. Grid – 10×20 finite elements.**

The following plate parameters were taken: $E$ = $10^7$ kN/m$^2$, $\mu$ = 0.21, $t$ = 0.1 m, $q$ = 10 kN/m$^2$. Sizes of the plate are shown in Figure 8. Calculations were performed for two finite element grids: 10 by 20 elements (Figure 8) and 20 by 40 elements. In addition, for comparison, calculations of this plate were performed using the LIRA-SAPR program. All results are given in Table 5.

***Table 5. Displacements and bending moments in the center of the plate (Figure 8).***

| Solution (grid) | $w$, mm | $M_x$, kN · m/m | $M_y$, kN · m/m |
|---|---|---|---|
| SFEM (10×20) | 9.074 | 3.371 | 8.635 |
| SFEM (20×40) | 9.187 | 3.437 | 8.780 |
| LIRA-SAPR (10×20) | 9.115 | 4.758 | 7.237 |
| LIRA-SAPR (20×40) | 9.149 | 4.828 | 7.347 |
| Timoshenko [29] | 9.719 | – | 8.712 |

The values of the bending moments in the plate center (for SFEM and for LIRA-SAPR) were determined as the middle value of moments in two elements adjacent to the center point on one half plate. Note that the moments in the two finite elements differ by about 5 percent. The bending moments obtained by the proposed method are close to the corresponding values given in [29], and the value of plate center displacement is less than the corresponding value given in [29] by about 6 %, but almost coincides with the value obtained using the LIRA-SAPR program. The results of the skew plate calculations show a good accuracy of the proposed method for calculating the Reisner's plates with using finite elements in the parallelogram form. Note that the plate under consideration is thin, but nevertheless the solution “locking” effect is absent, as well as for the plate in the semiring form from the previous example.

# 4. Conclusion

1. A method for calculating of bending plates based on Reisner's theory by the finite element method is proposed. The method is based on the fundamental principles of additional energy minimum and possible displacements. The necessary relations for an arbitrary quadrangular finite element are obtained. Mathematically, the transition from differential equilibrium equations of bent plates to algebraic equilibrium equations for nodes of finite element grid.

2. The bending moments, torques and shear forces are constant in the finite element area, which is necessary condition for ensuring the solution convergence, when the mesh is crushed.

3. The proposed calculation method allows both thick and thin plates to be calculated. There is no effect of solution “locking” for thin plates, which is confirmed by rectangular plates calculations with different support conditions of side and different ratios of thickness to plate sizes.

4. Comparison of solutions obtained by the proposed method for plates of various shapes with analytical solutions shows fast convergence and proposed method accuracy of calculating both thick and thin plates.

### References


1. Gallager, R. Metod konechnykh elementov. Osnovy [Finite element method The basics]. Moskow: Mir, 1984. 428 p.(rus)
2. Sekulovich, M. Metod konechnykh elementov [Finite element method]. Moskow: Stroyizdat, 1993. 664 p. (rus)
3. Timoshenko, S.P., Voynovskiy-Kriger, S. Plastiny i obolochki [Plates and shells]. Moskow: Nauka, 1966. 636 p. (rus)
4. Fallah, N. On the use of shape functions in the cell centered finite volume formulation for plate bending analysis based on Mindlin–Reissner plate theory. Computers & Structures. 2006. 84. Pp. 1664–1672.
5. Katili, I., Batoz, J.L., Maknun, I.J., Hamdouni, A., Millet, O. The development of DKMQ plate bending element for thick to thin shell analysis based on the Naghdi/Reissner/Mindlin shell theory. Finite Elements in Analysis and Design. 2015. 100. Pp. 12–27.
6. Khezri, M., Gharib, M., Rasmussen, K.J.R. A unified approach to meshless analysis of thin to moderately thick plates based on a shear-locking-free Mindlin theory formulation. Thin-Walled Structures. 2018. Pp. 161–179.
7. Mirsaidov, M.M., Abdikarimov, R.A., Vatin, N.I., Zhgutov, V.M., Khodzhayev, D.A., Normuminov, B.A. Natural oscillations of a rectangular plates with two adjacent edges clamped. Magazine of Civil Engineering. 2018. 82(6). Pp. 112–126. doi: 10.18720/MCE.82.11
8. Lalin, V.V., Rozin, L.A., Kushova, D.A. Variatsionnaya postanovka ploskoy zadachi geometricheski nelineynogo deformirovaniya i ustoychivosti uprugikh sterzhney [Variational statement of the plane problem of geometrically nonlinear deformation and stability of elastic rods]. Magazine of Civil Engineering. 2013. 36(1). Pp. 87–96. (rus) doi: 10.5862/MCE.36.11
9. Rozin. L.A. Zadachi teorii uprugosti i chislennyye metody ikh resheniya [Problems of the theory of elasticity and numerical methods for their solution]. Sankt-Peterburg: SPbGTU, 1998. 532 p. (rus)
10. Rozin, L.A. Metod konechnykh elementov v primenenii k uprugim sistemam [The finite element method as applied to elastic systems]. Moskow: Stroyizdat, 1977. 129 p. (rus)
11. Park. M., Choi. D.-H. A two-variable first-order shear deformation theory considering in-plane rotation for bending, buckling and free vibration analysis of isotropic plates. Applied Mathematical Modelling. 2018. 61. Pp. 49–71.
12. Kumara. R., Lala, A., Singhb, B.N., Singhc, J. New transverse shear deformation theory for bending analysis of FGM plate under patch load. Composite Structures. 2019. 208. Pp. 91–100.

13. Thai, H.-T., Choi, D.-H. Finite element formulation of various four unknown shear deformation theories for functionally graded plates. Finite Elements in Analysis and Design. 2013. 75. Pp. 50–61.
14. Doa, T.V., Nguyenb, D.K., Ducc, N.D., Doanc, D.H., Buie, T.Q. Analysis of bi-directional functionally graded plates by FEM and a new third-order shear deformation plate theory. Thin-Walled Structures. 2017. 119. Pp. 687–699.
15. Mulcahy, N.L., McGuckin, D.G. The addition of transverse shear flexibility to triangular thin plate elements. Finite Elements in Analysis and Design. 2012. 52. Pp. 23–30.
16. Karttunen, A.T., Hertzen, R., Reddy, J.N., Romanoff, J. Shear deformable plate elements based on exact elasticity solution. Computers & Structures. 2018. 200. Pp. 21–31.
17. Duan, H., Ma, J. Continuous finite element methods for Reissner-Mindlin plate problem. Acta Mathematica Scientia. 2018. 38. Pp. 450–470.
18. Sukhoterin, M.V., Baryshnikov, S.O., Knysh, T.P. Stress-strain state of clamped rectangular Reissner plates. Magazine of Civil Engineering. 2017. 76(8). Pp. 225–240. doi: 10.18720/MCE.76.20
19. Sukhoterin, M.V., Baryshnikov, S.O., Potekhina, Ye.V. O raschetah plastin po sdvigovym teoriyam [About plate calculations based on shear theories]. Vestnik gosudarstvennogo universiteta morskogo i rechnogo flota im. admirala, S.O. Makarova. 2015. 30(2). Pp. 81–89. (rus)
20. Zenkour, A.M. Exact mixed-classical solutions for the bending analysis of shear deformable rectangular plates. App. Math. Model. 2003. 27. Pp. 515–534.
21. Erkmen, R.E. Shear deformable hybrid finite-element formulation for buckling analysis of thin-walled members. Finite Elements in Analysis and Design. 2014. 82. Pp. 32–45.
22. Özütok, A., Madenci, E. Static analysis of laminated composite beams based on higher-order shear deformation theory by using mixed-type finite element method. International Journal of Mechanical Sciences. 2017. 130. Pp. 234–243.
23. Senjanović, I., Vladimir, N., Hadžić, N. Modified Mindlin plate theory and shear locking free finite element formulation. Mechanics Research Communications. 2014. 55. Pp. 95–104.
24. Tyukalov, Yu.Ya. Finite element models in stresses for plane elasticity problems. Magazine of Civil Engineering. 2018. 77(1). Pp. 23–37. doi: 10.18720/MCE.77.3
25. Tyukalov, Yu.Ya. The functional of additional energy for stability analysis of spatial rod systems. Magazine of Civil Engineering. 2017. 70(2). Pp. 18–32. doi: 10.18720/MCE.70.3
26. Tyukalov, Yu.Ya. Stress finite element models for determining the frequencies of free oscillations. Magazine of Civil Engineering. 2016. 67(7). Pp. 39–54. doi: 10.5862/MCE.67.5
27. Tyukalov, Yu.Ya. Finite element models in stresses for bending plates. Magazine of Civil Engineering. 2018. 82(6). Pp. 170–190. doi: 10.18720/MCE.82.16
28. Tyukalov, Yu.Ya. Calculation method of bending plates with assuming shear deformations. Magazine of Civil Engineering. 2019. 85(1). Pp. 107–122. doi: 10.18720/MCE.85.9
29. Donnell, L.G. Balki, plastiny i obolochki [Beams, plates and shells]. Moskow: Nauka, 1982. 568 p. (rus)
30. Belkin, A.Ye., Gavryushin, S.S. Raschet plastin metodom konechnykh elementov [Plate calculation by finite element method]. Moskow: MGTU, 2008. 231 p. (rus)


***Contacts:***

*Yury Tyukalov, +7(912)8218977; yutvgu@mail.ru*

Инженерно-строительный журнал

ISSN 2071-0305

сайт журнала: http://engstroy.spbstu.ru/

DOI: 10.18720/MCE.89.6

# Конечно-элементная модель в напряжениях для пластин Рейснера

***Ю.Я. Тюкалов***
*Вятский государственный университет, г. Киров, Россия*

**Ключевые слова:** пластины Рейсснера, возможные перемещения, конечные элементы, изгибаемые пластины

**Аннотация.** Предложена методика расчета изгибаемых пластин методом конечных элементов на основе теории Рейснера. Метод основывается на фундаментальных принципах минимума дополнительной энергии и возможных перемещений. Для дискретизации предметной области используются произвольные четырехугольные конечные элементы. По области конечного элемента поля моментов и поперечных сил аппроксимируются постоянными функциями, которые удовлетворяют дифференциальным уравнениям равновесия в области конечного элемента при отсутствии распределенной нагрузки. Используя принцип возможных перемещений, составляются алгебраические уравнения равновесия узлов сетки конечных элементов. При этом, в соответствии с теорией Рейсснера, в качестве узловых возможных перемещений принимаются, независимо, вертикальные перемещения и углы поворота срединной поверхности пластины. Предлагаемый метод расчета позволяет рассчитывать как толстые, так и тонкие пластины. Эффект «заклинивания» решения для тонких пластин отсутствует, что подтверждено расчетами прямоугольных пластин с различными условиями опирания и различными отношениями толщины к размеру пластины. Сравниваются решения, полученные по предлагаемой методике для пластин различной формы, с аналитическими решениями. Показана достаточно быстрая сходимость и точность предлагаемой методики расчета как для толстых, так и для тонких пластин.

## Литература

1. Галлагер Р. Метод конечных элементов. Основы. М.: Мир, 1984. 428 с.
2. Секулович М. Метод конечных элементов. М.: Стройиздат, 1993. 664 с.
3. Тимошенко С.П., Войновский-Кригер С. Пластины и оболочки. М.: Наука, 1966. 636 с.
4. Fallah N. On the use of shape functions in the cell centered finite volume formulation for plate bending analysis based on Mindlin–Reissner plate theory // Computers & Structures. 2006. Vol. 84. Pp. 1664–1672.
5. Katili I., Batoz J.L., Maknun I.J., Hamdouni A., Millet O. The development of DKMQ plate bending element for thick to thin shell analysis based on the Naghdi/Reissner/Mindlin shell theory // Finite Elements in Analysis and Design. 2015. Vol. 100. Pp. 12–27.
6. Khezri M., Gharib M., Rasmussen K.J.R. A unified approach to meshless analysis of thin to moderately thick plates based on a shear-locking-free Mindlin theory formulation // Thin-Walled Structures, 2018. Pp. 161–179.
7. Мирсаидов М.М., Абдикаримов Р.А., Ватин Н.И., Жгутов В.М., Ходжаев Д.А., Нормуминов Б.А. Нелинейные параметрические колебания вязкоупругой пластинки переменной толщины // Инженерно-строительный журнал. 2018. № 6(82). С. 112–126. doi: 10.18720/MCE.82.11
8. Лалин В.В., Розин Л.А., Кушова Д.А. Вариационная постановка плоской задачи геометрически нелинейного деформирования и устойчивости упругих стержней // Инженерно-строительный журнал. 2013. № 1(36). С. 87–96. doi: 10.5862/MCE.36.11
9. Розин Л. А. Задачи теории упругости и численные методы их решения. СПб.: СПбГТУ, 1998. 532 с.
10. Розин Л.А. Метод конечных элементов в применении к упругим системам. М.: Стройиздат, 1977. 129 с.
11. Park M., Choi D.-H. A two-variable first-order shear deformation theory considering in-plane rotation for bending, buckling and free vibration analysis of isotropic plates // Applied Mathematical Modelling. 2018. Vol. 61. Pp. 49–71.
12. Kumara R., Lala A., Singhb B.N., Singhc J. New transverse shear deformation theory for bending analysis of FGM plate under patch load // Composite Structures. 2019. Vol. 208. Pp. 91–100.
13. Thai H.-T., Choi D.-H. Finite element formulation of various four unknown shear deformation theories for functionally graded plates // Finite Elements in Analysis and Design. 2013. Vol. 75. Pp. 50–61.
14. Doa T.V., Nguyenb D.K., Ducc N.D., Doanc D.H., Buie T.Q. Analysis of bi-directional functionally graded plates by FEM and a new third-order shear deformation plate theory // Thin-Walled Structures. 2017. Vol. 119. Pp. 687–699.
15. Mulcahy N.L., McGuckin D.G. The addition of transverse shear flexibility to triangular thin plate elements // Finite Elements in Analysis and Design. 2012. Vol. 52. Pp. 23–30.

16. Karttunen A.T., Hertzen R., Reddy J.N., Romanoff J. Shear deformable plate elements based on exact elasticity solution // Computers & Structures. 2018. Vol. 200. Pp. 21–31.
17. Duan H., Ma J. Continuous finite element methods for Reissner-Mindlin plate problem // Acta Mathematica Scientia. 2018. Vol. 38. Pp. 450–470.
18. Сухотерин М.В., Барышников С.О., Кныш Т.П. Напряженно-деформированное состояние защемленной прямоугольной пластины Рейсснера // Инженерно-строительный журнал. 2017. № 8(76). С. 225–240. doi: 10.18720/MCE.76.20
19. Сухотерин М.В., Барышников С.О., Потехина Е.В. О расчетах пластин по сдвиговым теориям // Вестник государственного университета морского и речного флота им. адмирала С.О. Макарова. 2015. № 2 (30). С. 81–89.
20. Zenkour A.M. Exact mixed-classical solutions for the bending analysis of shear deformable rectangular plates // App. Math. Model. 2003. Vol. 27. Pp. 515–534.
21. Erkmen R.E. Shear deformable hybrid finite-element formulation for buckling analysis of thin-walled members // Finite Elements in Analysis and Design. 2014. Vol. 82. Pp. 32–45.
22. Özütok A., Madenci E. Static analysis of laminated composite beams based on higher-order shear deformation theory by using mixed-type finite element method // International Journal of Mechanical Sciences. 2017. Vol. 130. Pp. 234–243
23. Senjanović I., Vladimir N., Hadžić N. Modified Mindlin plate theory and shear locking free finite element formulation // Mechanics Research Communications. 2014. Vol. 55. Pp. 95–104.
24. Тюкалов Ю.Я. Конечно-элементные модели в напряжениях для задач плоской теории упругости // Инженерно-строительный журнал. 2018. № 1(77). С. 23–37. doi: 10.18720/MCE.77.3
25. Тюкалов Ю.Я. Функционал дополнительной энергии для анализа устойчивости пространственных стержневых систем // Инженерно-строительный журнал. 2017. № 2(70). С. 18–32. doi: 10.18720/MCE.70.3
26. Тюкалов Ю.Я. Определение частот свободных колебаний методом конечных элементов в напряжениях // Инженерно-строительный журнал. 2016. № 7(67). С. 39–54. doi: 10.5862/MCE.67.5
27. Тюкалов Ю.Я. Конечно элементные модели в напряжениях для изгибаемых пластин // Инженерно-строительный журнал. 2018. № 6(82). С. 170–190. doi: 10.18720/MCE.82.16
28. Тюкалов Ю.Я. Метод расчета изгибаемых плит с учетом деформаций сдвига // Инженерно-строительный журнал. 2019. № 1(85). С. 107–122. DOI: 10.18720/MCE.85.9
29. Доннелл Л.Г. Балки, пластины и оболочки. М.: Наука, 1982. 568 с.
30. Белкин А.Е., Гаврюшин С.С. Расчет пластин методом конечных элементов. М.: МГТУ, 2008. 231 с.


### *Контактные данные:*

*Юрий Яковлевич Тюкалов, +7(912)8218977; эл. почта: yutvgu@mail.ru*